Science in China Series B: Chemistry

Study of the interaction of unaggregated and aggregated amyloid β protein (10-21) with outward potassium channel

ZHANG ChaoFeng, FAN Li & YANG Pin†

Key Laboratory of Chemical Biology and Molecular Engineering of Ministry of Education, Institute of Molecular Science, Shanxi University, Taiyuan 030006, China

Metal ion-induced aggregation of Aβ into insoluble plaques is a central factor in Alzheimer's disease. Zn^{2+} is the only physiologically available transition metal ion responsible for aggregating Aβ at pH 7.4. To make it clear that the neurotoxicity of Zn^{2+}-induced aggregation of Aβ on neurons is the key to understand Aβ mechanism of action further. In this paper, we choose Aβ (10-21) as the model fragment to research hippocampal CA1 pyramidal neurons. For the first time, we adopt the combination of spectral analysis with patch-clamp technique for the preliminary study of the mutual relations of Zn^{2+}, Aβ and ion channel from the cell level. The following expounds upon the effects and mode of action of two forms (unaggregated and aggregated) of Aβ (10-21) on hippocampus outward potassium channel three processes (activation, inactivation and reactivation). It also shows the molecular mechanics of AD from the channel level. These results are significant for the further study of Aβ nosogenesis and the development of new types of target drugs for the treatment of AD.

potassium channel, amyloid β protein (10-21), Zn^{2+}, alzheimer's disease

Alzheimer's disease (AD) is the most common form of dementia in the elderly population. It is clinically characterized by a progressive loss of cognitive abilities, progressive memory and intellectual deficits[1]. This disease debilitates millions of elderly people and presents an enormous burden on the families of those affected, as well as society in general. The cause of AD is closely related to the aggregation of a normal protein, β-amyloid (Aβ), within the neocortex. Aβ peptide is generated from amyloid precursor protein by the proteolytic activity of β-and γ-secretase[2]. Aβ has been described in three biochemical fractions in the brain: membrane associated, aggregated and soluble. In healthy individuals, most of the Aβ is membrane associated, but in individuals with AD the aggregated (diffuse and plaque amyloid) and soluble fractions increase markedly[3]. Although the mechanism leading to the aggregation of this normally soluble protein is not fully understood, more and more evidence has been gathered to suggest that Aβ precipitation and toxicity in AD are caused by abnormal interactions with neocortical metal ions, especially Zn, Cu and Fe. These transition metal ions are highly concentrated in the neocortical regions most effected in AD[4] and also found at high levels in amyloid plaques (Zn^{2+}, 1055 μmol/L; Cu^{2+}, 390 μmol/L; Fe^{3+}, 940 μmol/L), compared with normal age-matched neuropil (Zn^{2+}, 350 μmol/L; Cu^{2+}, 70 μmol/L, Fe^{3+}, 340 μmol/L)[3]. Zn^{2+} appears to be the major neurochemical factor responsible for aggregating Aβ. *In vitro,* Aβ specifically interacts with Zn^{2+}, and Zn^{2+} drastically accelerates the Aβ aggregation[5,6]. Zn^{2+} is the only physio-

Received November 14, 2006; accepted December 18, 2006
doi: 10.1007/s11426-007-0049-1
†Corresponding author (email: yangpin@sxu.edu.cn)
Supported by the National Natural Science Foundation of China (Grant Nos. 30470408 and 20637010)

logically available metal ion to precipitate A β at pH 7.4[5,7], and Cu^{2+} (and Fe^{3+} to a lesser extent) induces limited Aβ aggregation[7], which is exaggerated by slightly acidic conditions. Experiments indicate that there are two binding sites for Zn^{2+} with A β (1-40): One is the high affinity site (K_D = 107 nmol/L); the other is the low affinity site (K_D = 5.2 μmol/L)[5]. In recent years, a series of intensive studies of the Zn^{2+}-A β interactions have been made by a range of complementary spectroscopies, such as NMR, Raman spectroscopy, EPR spectroscopy and CD. Zn^{2+}-induced aggregation of Aβ appears to be initiated by Zn^{2+} coordination with charged residues within the amino acid region 6-28 of Aβ [6]. While the histidine residues at positions 6, 13, and 14 of full length Aβ (1-42) have been implicated in metal binding, 13 and 14 appear to be most critical[8,9]. In the present experiment, we choose Aβ (10-21) as a model for use in Zn^{2+}-induced aggregation of Aβ. The value of Aβ (10-21) as an *in vitro* model has been strengthened by our group[10,11] and another group[8].

A key to understand the action of Aβ in AD is to determine how this protein affects the neuronal networks in which memories are stored, thereby causing dementia[12]. It is widely believed that the cellular actions of Aβ are responsible for the neurodegeneration observed in AD. A growing body of evidence indicates that Aβ has modulatory effects on ion channel currents in central neurons. The neurotoxic disruption of intracellular ion homeostasis may be the result of an action by Aβ on ion channel activity[13]. Both voltage-gated potassium and calcium channels have been implicated in these Aβ -induced changes. Two studies[14,15] have shown that Aβ can cause apoptotic cell death via an increase in the delayed rectifier K^+ channel current. In contrast to these two studies, Chen et al.[16] and Ye et al.[17] reported that Aβ inhibit specially A-type K^+ current but not other outward or inward rectifying K^+ channels. All peptides used in the earlier studies were aggregated by higher temperatures and longer incubate time and no experiments with the Zn^{2+}-induced aggregated form of Aβ were carried out. In addition, no characterization was presented to indicate the actual assembly state of the Aβ and no experiments with unaggregated form were carried out. The aim of this study, therefore, was to compare the effects of both unaggregated and aggregated forms of Aβ (10-21) on outward potassium channel (activation, inactivation and reactivation processes) in hippocampal CA1 pyramidal neurons. To this end, we have applied unaggregated and aggregated (induced by Zn^{2+}) forms of Aβ to hippocampal pyramidal neurons through combining spectral analysis with patch-clamp technique in order to determine the effects of each on the outward potassium channel currents in these cells.

1 Experimental

1.1 Isolation of hippocampal neurons

Single rat hippocampal pyramids neurons were acutely isolated by enzymatic digestion and mechanical dispersion from 7-day-old Wistar rats as previously described[18]. Hippocampal CA1 region was cut into 300－500 μm thick slices and incubated for 30 min at 32℃ in artificial cerebrospinal solution (ACS) and successively transferred into ACS containing 0.5 mg/mL protease and digested at 32℃ for 35 min. Throughout the entire procedure the media were continuously saturated with a 95% O_2-5% CO_2 gas mixture to maintain a pH of 7.4. After digestion, the tissue pieces were washed 3－4 times with ACS and neurons were triturated through a series of fire-polished glass pipettes with opening diameter from 0.1 to 0.5 mm. The cell suspension was transferred into a 35 mm culture dish filled with 1.5 mL extracellular solution. Twenty minutes later, the neurons were attached to the bottom of the culture dish and were ready for experiments.

1.2 Patch-clamp recording

According to the previous experiments[11,19], the pyramidal neurons with a diameter of 15–30 μm were identified by their characteristic bright pyramid-shaped soma under a phase contrast microscope and two or three short-branched dendrites and a long axon. The patch electrodes (BJ-40, diameter 1.5±0.1mm, Beijing) were pulled in two steps by a microeletrode puller (PP-830, Narrishage, Japan) and had tip resistance of 5－8 MΩ when filled with pipette solution. Whole-cell currents were recorded with Axopatch 200B patch clamp amplifier (Axon Instrument, USA). After forming a conventional "gigaseal", the membrane was ruptured with a gentle suction to obtain the whole-cell voltage clamp configuration. Liquid junction potential between the pipette solution and extracellular solution was compensated after the pipette tipped into the external solu-

tion.

1.3 Application of amyloid β protein (10—21)

Aβ (10-21) was purchased from Chinese Peptide Company. Stock peptide was stored as powder at −70℃. Stock solution of Aβ (10-21) was prepared by dissolving the peptides at a concentration of 1 mmol/L in deoxygenated, deionized water, aliquoted to 100 μL, and stored at −20℃ until needed. The concentration of peptide was determined from the UV absorption intensity of tyrosine (ε_{275} = 1410 L·mol^{-1}·cm^{-1}) at pH 7.4[20]. In most experiments, unaggregated Aβ (10-21) was added to bath solution for external application. For Zn^{2+}-induced aggregation experiments, peptide was prepared by dilution stock solution into 20 mmol/L sodium phosphate buffer. Peptide solution (100 μmol/L) containing different concentrations of Zn^{2+} was incubated for 0—24 h at 37℃ and then centrifuged (5415D, Eppendorf) at 13000 *g* for 10 min. Peptide concentrations, relative to uncentrifuged control without Zn^{2+}, were determined by fluorescamine assay[9]. Aggregation (%) = 100 − [(centrifuged value/uncentrifuged value) ×100]. For the fluorescamine assay, an F-2500 fluorometer with a 390 nm excitation wavelength filter and a 480 nm emission filter was used.

1.4 Preparation of experimental solutions (mmol/L)

Sodium phosphate buffer: NaH_2PO_4-Na_2HPO_4 20, NaCl 150, pH 7.4. Artificial cerebrospinal solution (ACS): NaCl 124, KCl 5, KH_2PO_4 1.2, $MgSO_4$ 1.3, $CaCl_2$ 2.4, glucose 10, $NaHCO_3$ 26, pH adjusted to 7.4 with tris. Extracellular solution: NaCl 150, KCl 5, $MgCl_2$ 1.1, $CaCl_2$ 2.6, glucose 10, HEPES 10, pH adjusted to 7.4 with tris. To record potassium current, 1 μmol/L TTX and 0.2 mmol/L $CdCl_2$ were added to extracellular solution before the electrophysiological recording. Pipette solution: KCl 65, KOH 5, KF 80, $MgCl_2$ 2, HEPES 10, EGTA 10, Na_2ATP 2, pH adjusted to 7.3 with KOH. Protease, NaCl, TEA-Cl, HEPES, TTX were purchased from Sigma Company.

1.5 Analysis of electrophysiological recordings

Currents were amplified by using an amplifier (Axopath 200B), and digidata 1200B interface (Axon Instrument, USA) and Pclamp version 6.0.4 software (Axon Instrument, USA) were used to produce protocols, and acquire and process data. All data were analyzed by the use of Clampfit procedures (Axon Instrument, USA) and MICROCAL-ORIGIN (5.0). All values were presented as mean ± S.D., and statistical comparisons were made using the paired student's *t*-test with $P < 0.05$ being statistically significant.

2 Results

2.1 Identification of outward potassium current

A depolarizing prepulse to 60 mV from a holding potential of −100 mV was followed by test pulse from −140 to −20 mV activated tail current of outward potassium current (Figure 1(a)). The membrane potential is often called reverse potential (E_{rev}) when ion channels tail current is at zero. Under the imposed ionic conditions, reverse potential was close to the theoretical equilibrium potential for the permeable ion. Figure 1(b) shows current-voltage relationship of tail currents with its data acquired from the experiment performed as in Figure 1(a). According to Figure 1(b), the reverse potential is −80 mV. K^+ equilibrium potential was calculated by Nernst equation $E_{rev} = (-2.303\ RT/zF) \times \lg([K^+]_i/[K^+]_o)$, where $[K^+]_i$, $[K^+]_o$ is K^+ concentration used in the extracellular solution and in the pipette solution, respectively. The K^+ equilibrium potential (−87 mV) was

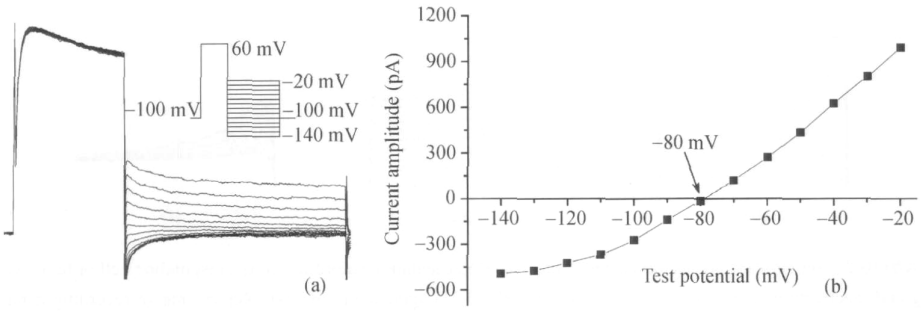

Figure 1 Outward potassium channel tail current (a) and current-voltage curve (b) of tail current.

nearly equal to reverse potential. This current was identified as outward potassium current further by tail currents analysis.

2.2 Separation of I_A and I_K

There are two components of outward current in hippocampal neurons: first, a rapidly activating and inactivating current, sensitive to 4-AP, referred to as I_A; and then a delayed rectifier current, sensitive to TEA, named as I_K. To study the effects of lithium chloride on I_A and I_K respectively, a signal subtraction procedure was used to separate I_K from the total potassium current. Step depolarization to potential from –50 to +60 mV following a hyperpolarizing prepulse of 400 ms to –110 mV clearly activated two components of outward current (Figure 2(a)). By holding at –50 mV and stepping to more positive potentials, I_A undergoes steady-state inactivation; therefore, I_K could be activated nearly uncontaminated with I_A[21]. With this protocol, I_K was activated slowly to a plateau with minimal time-dependent inactivation (Figure 2(b)). Subtraction of I_K from total potassium current revealed I_A (Figure 2(c)). Currents at the end of the depolarizing pulse were referred to as I_K. The peak of the subtracted currents was referred to as I_A.

2.3 Effects of unaggregated Aβ(10-21) on I_A and I_K

To determine the potential effects of unaggregated Aβ(10-21) on two components of outward potassium current, Aβ(10-21) of various concentrations was added to the extracellular solution at final concentrations of 1×10^{-5}, 2×10^{-5}, 3×10^{-5}, 5×10^{-5} mol/L. Figures 2(d), (e), and (f) respectively showed the whole-cell currents of total potassium, I_K and I_A after the application of 1×10^{-5} mol/L Aβ(10-21). It is showed that Aβ(10-21) decreased the amplitudes of I_A drastically (Figure 2(f)), but the amplitudes of I_K were not affected (Figure 2(e)). In addition, upon the administration of Aβ(10-21) (in μmol/L): 10, 20, 30, 50, there was a decrease in the amplitudes of I_A, and this action progressed incrementally in concentrations from 10 to 50 (Figure 3). The results indicated that Aβ(10-21) decreased the amplitudes of I_A in a concentration-dependent manner. At the concentration of 50 μmol/L, Aβ(10-21) inhibited I_A by (36.93± 0.65) % ($n=3$, $P<0.01$) at 60 mV.

2.4 Zn^{2+}-induced aggregation of Aβ(10-21)

Aβ(10-21) itself has no fluorescence, and yields intense fluorescence when it combines with fluorescamine, a

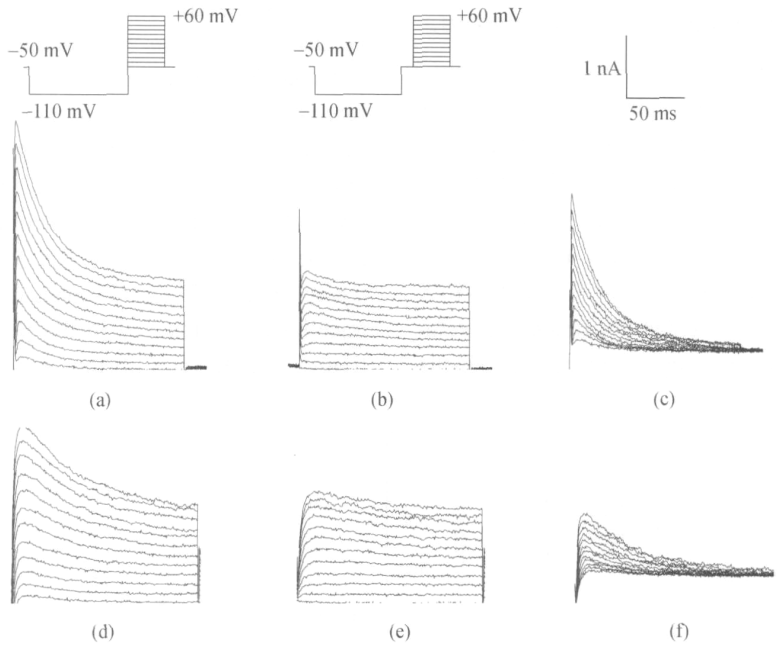

Figure 2 Effect of Aβ(10-21) on outward potassium currents. (a)—(c) Representative recording from a responding cell of total (a), delayed rectifier (b) and rapidly activating and inactivating (c) potassium current before Aβ(10-21) application. (d)—(f) Representative recording from a responding cell of total (a), delayed rectifier (b) and rapidly activating and inactivating (c) potassium current after Aβ(10-21) application. The command potentials used to evoke total and delayed rectifier currents are shown.

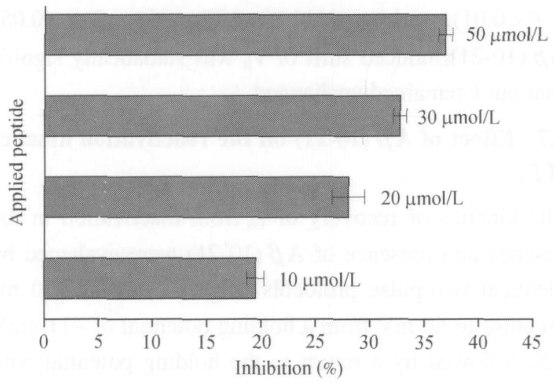

Figure 3 Effect of Aβ(10-21) is concentration-dependent.

nonfluorescent compound. The fluorescent intension of Aβ(10-21) derivative will weaken when it is aggregated partly by metal ions. Thus, fluorescamine provides a new tool for the assay of peptides at a level which were hitherto out of reach. In the present experiment, Aβ(10-21) did not aggregate significantly and was stable for months in aqueous in the absence of Zn^{2+}. In the presence of Zn^{2+}, Aβ(10-21) aggregated rapidly and this action progressed incrementally in Zn^{2+} concentrations from 0 to 10 μmol/L (Figure 4), which showed that Zn^{2+} induced Aβ(10-21) aggregation in a concentration-dependent manner. These results indicate that Aβ(10-21) can be used as an *in vitro* model in Zn^{2+}-induced Aβ aggregation and that the region 10-21 can be the minimal fragment of zinc-binding domain of full length Aβ(1-42).

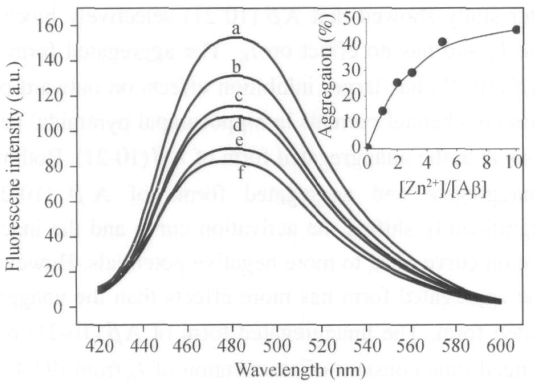

Figure 4 Zn^{2+}-induced aggregation of Aβ(10-21).

2.5 Effects of aggregated Aβ(10-21) on I_A and I_K

The aim of this section was to compare the effects of both unaggregated and aggregated forms of Aβ(10-21) on outward potassium channel in central neurons. To this end, we have applied unaggregated and aggregated forms of Aβ(10-21) to hippocampal pyramidal neurons in order to determine the effects of each on the voltage-gated potassium channel currents in these cells. In the unaggregated form, Aβ(10-21) inhibited I_A by (19.50±0.81)% (n=3). In the aggregated form, Aβ(10-21) inhibited I_A by (45.93±0.99)% (n=3) in the acute application (Figure 5(a)), indicating that aggregation form of Aβ(10-21) had larger modulatory effects on potassium channel currents than the unaggregated form. Figure 5(b) showed current-voltage (I-V) curves of I_A generated by depolarizing steps from a holding potential of −50 to +60 mV with a 10 mV increment. The inhibition of I_A was obvious ($P < 0.05$) only at potentials more positive than 0 mV, which could be attributed to electrostatic interaction of Aβ(10-21) with the membrane[22].

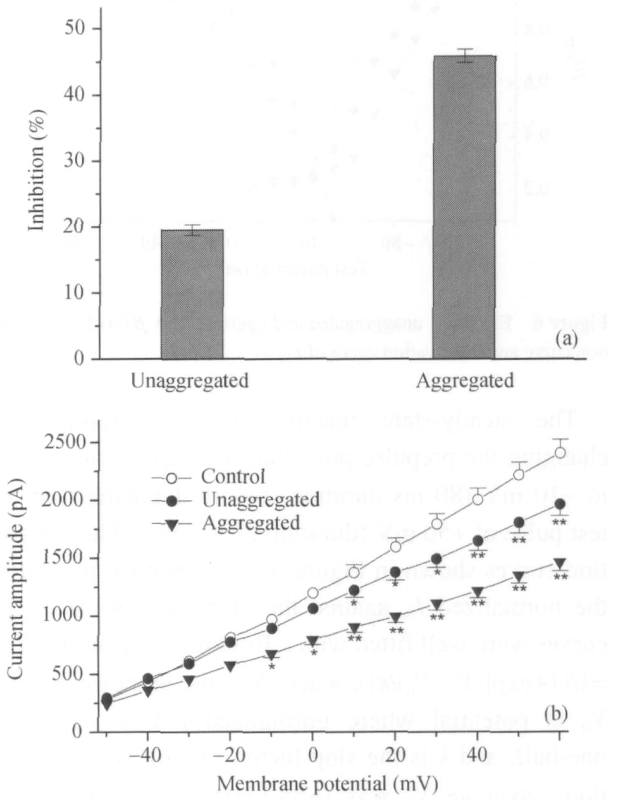

Figure 5 Effects of unaggregated and aggregated Aβ(10-21) on I_A (a) and current-voltage curve of I_A (b).

2.6 Effect of Aβ(10-21) on the activation and inactivation kinetics of I_A

I_A was converted into conductance by use of the equa-

tion $G=I/(V-V_K)$, where G is conductance, V is membrane potential, and V_K is reversal potential. With the least-squares fit procedure, the normalized conductance was well fitted with a Boltzmann equation: $G/G_{max} = 1/(1+\exp[-(V-V_h)/k])$, where G_{max} is the maximum conductance, V_h is the voltage at which half-maximal effect is obtained, and k is the slope factor (Figure 6). Before application of Aβ(10-21), the value of V_h was (–20.31±1.87) mV and k was (34.68±4.66) mV. Aβ(10-21) (10 μmol/L) caused a negative shift of the activation curve along the potential axis. The values of V_h for unaggregated and aggregated Aβ(10-21) were (–30.09±2.93) and (–32.26±2.05) mV (n=6, $P < 0.01$), with k of (20.49±1.30) and (11.68±0.92) mV (n=6, $P < 0.01$), respectively.

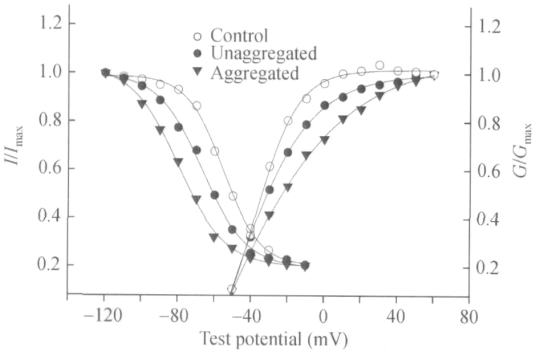

Figure 6 Effects of unaggregated and aggregated Aβ(10-21) on activation curve and inactivation curve of I_A.

The steady-state inactivation was examined by changing the prepulse potentials at levels between –120 to –10 mV (80 ms duration) before depolarization to a test pulse of +50 mV (duration of 120 ms). The inactivation curves shown in Figure 6 were obtained by plotting the normalized I_A against the prepulse potentials. The curves were well fitted with a Boltzmann equation: $I/I_{max} = 1/(1+\exp[(V-V_h)/k])$, where V is the prepulse potential, V_h is potential where normalized I was reduced to one-half, and k is the slop factor. During control conditions, average V_h was (–55.13±0.56) mV and k was (10.06±0.51) mV. After the addition of 10 μmol/L unaggregated Aβ(10-21), the inactivation curve was shifted to negative potentials: V_h was (–66.63±1.91) mV (n=6, $P<0.01$), and k was (12.20±0.89) mV (n=6, $P>0.05$). Aggregated Aβ(10-21) shifted the inactivation curve to more negative potentials: V_h was (–79.73±0.86) mV (n=5, $P<0.01$), and k was (12.89±0.78) mV (n=5, $P>0.05$). Aβ(10-21) induced shift of V_h was statistically significant but k remained unchanged.

2.7 Effect of Aβ(10-21) on the reactivation kinetics of I_A

The kinetics of recovery of I_A from inactivation in the absence and presence of Aβ(10-21) were evaluated by identical two-pulse protocols (Figure 7(a)). A 400 ms prepulse to 60 mV from a holding potential of –110 mV was followed by a return to the holding potential with variable duration (Δt) and then by a 400 ms test pulse to 60 mV. Selected I_A reactivation traces from a typical experiment in the absence and presence of Aβ(10-21) are shown in Figure 7(b) and (c). The magnitude of peak I_A elicited by the second pulse was expressed as a function of I_A during the first pulse and plotted against the interpulse duration (Figure 7(d)). The time course of recovery (τ_{rec}) from inactivation of I_A was fitted by a monoexponential function. Under control condition, the time constant of I_A was (93.43±5.45) ms (n=3). In the presence of Aβ(10-21) (1×10^{-5} mol/L), τ_{rec} was (115.06±10.63) ms (n=3) for unaggregated Aβ(10-21), and (132.11±5.00) ms (n=3) for aggregated Aβ(10-21). These results indicated that Aβ(10-21) prolonged recovery from inactivation of hippocampal potassium channel.

3 Conclusions and discussion

Our study showed that Aβ(10-21) selectively blocked the I_A and has no effect on I_K. The aggregated form of Aβ(10-21) has larger inhibition effects on outward potassium channel currents in hippocampal pyramidal neurons than the unaggregated form of Aβ(10-21). Both the unaggregate and aggregated forms of Aβ(10-21) significantly shifted the activation curve and the inactivation curve of I_A to more negative potentials. However, the aggregated form has more effects than the unaggregated form. The unaggregated form of Aβ(10-21) prolonged time constant of reactivation of I_A from (93.43±5.45) to (115.06±10.63) ms. In the aggregated form, Aβ(10-21) prolonged time constant of reactivation of I_A to (132.11±5.00) ms (Table 1). These results indicated that Zn^{2+}-induced aggregation of Aβ(10-21) potentiates its modulatory effects on potassium channel currents.

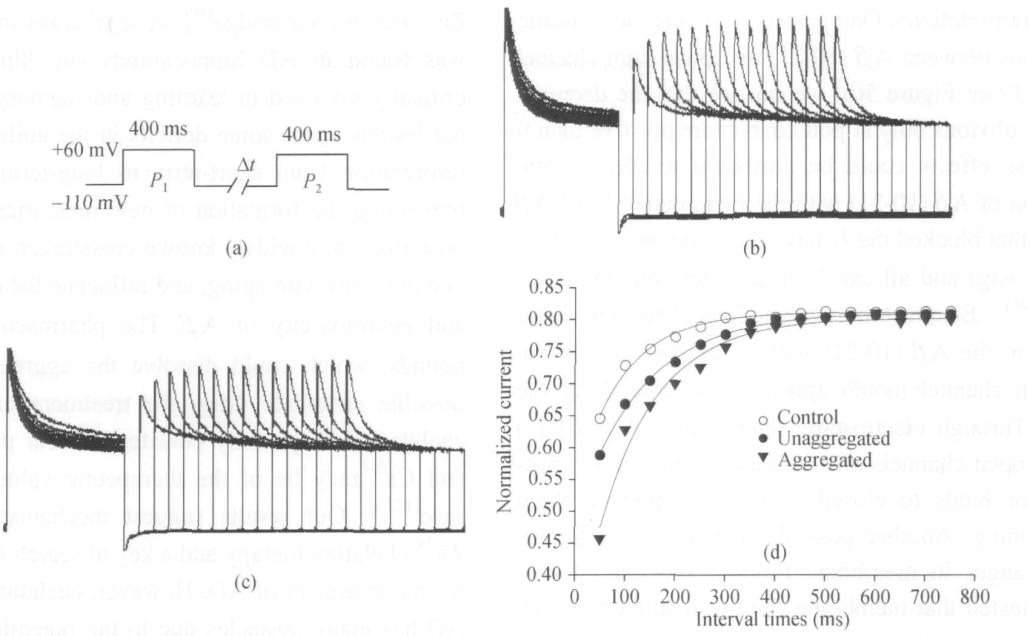

Figure 7 Effects of A β (10-21) on reactivation curve of I_A. (a) Two-pulse protocol; superimposed recording of I_A recovery from inactivation from the same cell are shown before (b) and after (c) application of A β (10-21); (d) the time course of recovery of I_A from inactivation. Data fit with a mono-exponential process.

Table 1 Effects of A β(10-21) on activation, inactivation and reactivation processes of I_A

System	Activation	Inactivation	Reactivation
Control	V_h (−20.31±1.87) mV	V_h (−55.13±0.56) mV	τ_{rec} (93.43±5.45) ms
	k (34.68±4.66) mV	k (10.06±0.51) mV	
Unaggregated A β(10-21)	V_h (−30.09±2.93) mV (n=6)[a)]	V_h (−66.63±1.91) mV (n=6)[a)]	τ_{rec}(115.0±10.63) ms (n=3)[a)]
	k (20.49±1.30) mV (n=6)[a)]	k (12.20±0.89) mV (n=6)[b)]	
Aggregated A β(10-21)	V_h (−32.26±2.05) mV (n=6)[a)]	V_h (−79.73±0.86) mV (n=5)[a)]	τ_{rec}(132.11±5.00) ms (n=3)[a)]
	k (11.68±0.92) mV (n=6)[a)]	k (12.89±0.78) mV (n =5)[b)]	

a) P<0.01; b) P<0.05.

Potassium channels play crucial roles in regulating a variety of cellular processes in both excitable and non-excitable cells, such as setting the membrane potential, action potential duration, the delay between a stimulus and the first action potential, discharge patterns, etc[23]. Blockage of potassium channels in hippacampal neurons causes Ca^{2+} influx through voltage-dependent channels and the *N*-methyl-*D*-aspartate receptor[24]. It has been shown that Aβ increase cell excitability and causes a rise in intracellular Ca^{2+} in hippocampal neurons[25] and that K^+ channels openers protect hippocampal neurons against oxidative injury and Aβ toxicity, presumably because of their ability to hyperpolarize the plasma membrane and reduce Ca^{2+} influx[26]. A transient increase of intracellular Ca^{2+} mediates information-coding processes in neural circuits and regulates growth cone behaviors in developing neurons. However, uncontrolled prolonged elevation of intracellular Ca^{2+} can result in neuronal degeneration and cell death by multiple pathways, including induction of apoptosis, damage of cellular proteins and membranes，and promotion of free radical production[27]. Thus, we hypothesize that Aβ-induced neurotoxicity is initiated by blockage of I_A channels, resulting in membrane depolarization, leading to increased Ca^{2+} influx, intracellular Ca^{2+} accumulation, thus beginning a cascade of subsequent cellular responses that eventually result in neuronal dysfunction and death[28].

The above conclusions indicated that Aβ(10-21) alter cellular ionic activity through interaction with existing ion channels in the membrane. This is consistent with early report[29]. Although the mechanism by which Aβ(10-21) affect hippocampal potassium channels is not clear at this time, we considered that there are two po-

tential interpretations. One possibility is the electrostatic interactions between Aβ(10-21) and potassium channel proteins. From Figure 5(b) we can see that the decrease of I_A was obvious only at potentials more positive than 0 mV. These effects could be attributed to electrostatic interaction of Aβ(10-21) with the membrane[22]. All Aβ peptides that blocked the I_A have the same basic residues (Lys and Arg) and all can form β-sheet containing aggregates[28]. Electrostatic interactions between basic residues in the Aβ(10-21) with acidic residues in the potassium channel mouth appear to be crucial for the affinity. Through electrostatic interactions, Aβ(10-21) binds to open channels and increases their rate of inactivation or binds to closed channels to prevent them from opening. Another possible mechanism might involve changes in membrane fluidity. Previous studies have indicated that membrane fluidity is altered in AD. Aβ can decrease membrane fluidity in a concentration-dependent fashion[30]. It is suggested that the small changes of membrane fluidity seen in the presence of unaggregated form of Aβ(10-21) may be sufficient to alter properties and functions of membrane-associated ionic channels. At aggregated form, Aβ(10-21) seem to have more pronounced effects on membrane fluidity, probably by disrupting membrane integrity, and directly leading to its neurotoxic properties[11].

We also noticed that without the addition of Zn^{2+}, the stock solution of Aβ(10-21) dissolved in deoxygenated, deionized water can keep for months and did not aggregate significantly. In the presence of Zn^{2+}, Aβ(10-21) aggregated rapidly through intermolecular His13 (N_τ)-Zn^{2+}-His14 (N_τ) bridge[10]. A significant increase in Zn was found in AD hippocampus and hippocampus is critically involved in learning and memory. Hippocampal lesions cause some deficits in the ability to transfer information from short-term to long-term stores, thus preventing the formation of new memories[31]. We propose that Zn, a widely known crosslinker, may accumulate in brains with aging, and influence the conformation and neurotoxicity of Aβ. The pharmacological compounds, which could dissolve the aggregated Aβ are possible candidate drugs for treatment of AD. Metal chelators that specially chelate Zn^{2+} but preserve Mg^{2+} and Ca^{2+} may be of the therapeutic value in AD disease[32,33]. Our results suggest mechanisms based on Zn^{2+}-chelation therapy and a key to search for new drugs for the treatment of AD. However, chelation therapy for AD has many obstacles due to the potential difficulties in reaching the target brain tissue (due to the blood-brain barrier), route of administration, possible associated nonspecific problems of systemic metal ion depletion, and potential severe side effects[4,33].

In conclusion, our findings, as well as results obtained from numerous biochemical and neurochemical studies about the link between Zn and AD, support the hypothesis that Zn may play a role as a co-factor in the pathogenesis of AD. Our study suggested that a neurotoxic disruption of intracellular ion homeostasis may be the result of an action by Aβ on potassium channel activity, and aggregation of Aβ had larger toxic effects on hippocampal neurons.

1 Penke B, Datki Z, Hetényi C, Molnár Z, Lengyel L, Soós K. Molecular pathomechanism of Alzheimer's disease. J Mol Struct, 2003, 666-667: 507－513

2 Checler F. Processing of the β-amyloid precursor protein and its regulation in Alzheimer's disease. J Neurochem, 1995, 65: 1431－1444

3 Bush A I. The metallobiology of Alzheimer's disease. Trends Neurosci, 2003, 26(4): 207－214

4 Cuajungco M P, Faget K Y. Zinc takes the center stage: Its paradoxical role in Alzheimer's disease. Brain Res Brain Res Rev, 2003, 41: 44－56

5 Bush A I, Pettingell W H, Multhaup G, Paradis M D, Vonsattel J P, Gusella J F, Beyreuther K, Masters C L, Tanzi R E. Rapid induction of Alzheimer's A beta amyloid formation by zinc. Science, 1994, 265: 1464－1467

6 Bush A I, Pettingell W H, Paradis M D, Tarzi R E. Modulation of A beta adhesiveness and secretase site cleavage by zinc. J Biol Chem, 1994, 269: 12152－12158

7 Atwood C S, Moir R D, Huang X, Scarpa R C, Bacarra N M E, Romano D M, Hartshorn M A, Tanzi R E, Bush A I. Dramatic aggregation of Alzheimer's Aβ by Cu(II) is induced by conditions representing physiological acidosis. J Biol Chem, 1998, 273(21): 12817－12826

8 Morgan D M, Dong J, Jacob J, Lu K, Apkarian R P, Thiyagarajan P, Lynn D G. Metal switch for amyloid formation: Insight into the structure of the nucleus. J Am Chem Soc, 2002, 124: 12644－12645

9 Liu S, Howlett G, Barrow C J. Histidine-13 is a crucial residue in the zinc ion-induced aggregation of the Aβ peptide of Alzheimer's disease. Biochemistry, 1999, 38: 9373－9378

10 Han D X, Yang P. Molecular modeling on Zn(II) binding modes of Alzheimer's amyloid β-peptide in insoluble aggregates and soluble complex. Sci China Ser B-Chem (in Chinese), 2004, 48: 126－133

11 Zhang C F, Yang P. Zinc-induced aggregation of Aβ(10-21) potentiates its action on voltage-gated potassium channel. Biochem Biophys

Res Commun, 2006, 345: 43－49
12 Small D H, Mok S S, Bornstein J C. Alzheimer's disease and Aβ toxicity: From top to bottom. Nat Rev Neurosci, 2001, 2: 595－597
13 Ramsden M, Plant L D, Webster N J, Vaughan P F, Henderson Z, Pearson H A. Differential effects of unaggregated and aggregated amyloid β protein (1-40) on K channel currents in primary cultures of rat cerebelllar granule and cortical neurons. J Neurochem, 2001, 79: 699－712
14 Colom L V, Diaz M E, Beers D R, Neely A, Xie W J, Appel S H. Role of potassium channels in amyloid-induced cell death. J Neurochem, 1998, 70: 1925－1933
15 Yu S P, Farhangrazi Z S, Ying H S, Yeh C H, Choi D W. Enhancement of outward potassium current may participate in β-amyloid peptide induced cortical neuronal death. Neurobiol Dis, 1998, 5: 81－88
16 Chen C. β-amyloid increases dendritic Ca^{2+} influx by inhibiting the A-type K^+ current in hippocampal CA1 pyramidal neurons. Biochem Biophys Res Commun, 2005, 38: 1913－1919
17 Ye C P, Selke D J, Hartley D M. Protofibrils of amyloid β-protein inhibit specific K^+ currents in neocortical cultures. Neurobiol Dis, 2003, 13: 177－190
18 Meng Z Q, Nie A F. Effects of sodium metabisulfite on potassium currents in acutely isolated CA1 pyramidal neurons of rat hippocampus. Food Chem Toxicol, 2005, 43: 225－232
19 Zhang C F, Du H Z, Yang P. Effects of lithium chloride on outward potassium currents in acutely isolated hippocampal CA1 pyramidal neurons. Chin Sci Bull, 2006, 51(16): 1961－1966
20 Miura T, Suzuki K, Kohata N, Takeuchi H. Metal binding modes of alzheimer's amyloid β-peptide in insoluble aggregates and soluble complexes. Biochemistry, 2000, 39: 7024－7031
21 Pan Y P, Xu X H, Wang X L. Galantamine blocks delayed rectifier, but not transient outward potassium current in rat dissociated hippocampal pyramidal neurons. Neurosci Lett, 2002, 336: 37－40
22 Hertel C, Terzi E, Hauser N, Jakob-Rotne R, Seeling J, Kemp J A. Inhibition of electrostatic interaction between β-amyloid peptide and membranes prevents β-amyloid- induced toxicity. Proc Natl Acad Sci USA, 1997, 94: 9412－9416
23 Storm J F. Potassium currents in hippocampal pyramidal cells. Brain Res, 1990, 83: 161－187
24 Le W D, Colom L V, Xie W J, Smith R G, Alexiann M, Appel S H. Cell death induced by β-amyloid (1-40) in MES 23.5 hybrid clone: The role of nitric oxide and NMDA-gated channel activation leading to apoptosis. Brain Res, 1995, 686: 49－60
25 Brorson J R, Bindokas V P, Lwama T, Marcuccilli C J, Chisholm J C, Miller R J. The Ca^{2+} influx induced by β-amyloid peptide 25-35 in cultured hippocampal neurons results from network excitation. J Neurobiol, 1995, 26: 325－338
26 Goodman Y, Mattson M P. K^+ channel openers protect hippocampal neurons against oxidative injury and amyloid β-peptide toxicity. Brain Res, 1996, 706: 328－332
27 Yagamia T, Ueda K, Sakaeda T, Itoh N, Sakaguchi G, Okamura N, Hori Y, Fujimoto M. Protective effects of a selective L-type voltage-sensitive calcium channel blocker, S-312-d, on neuronal cell death. Biochem Pharmacol, 2004, 67: 1153－1165
28 Good T A, Smith D O, Murphy R M. β-Amyloid peptide blocks the fast-inactivating K^+ current in rat hippocampal neurons. Biophys J, 1996, 70: 296－304
29 Fraster S P, Suh Y H, Djamgoz M B A. Ionic effects of the Alzheimer's disease β-amyloid precursor protein and its metabolic fragments. Trends Neurosci, 1997, 20: 67－72
30 Muller W E, Koch S, Eckert A, Hartmann H, Eckert A. β-Amyloid peptide decrease membrane fluidity. Brain Res, 1995, 674: 133－136
31 Wu W W, Matthew Oh M, Disterhoft J F. Age-related biophysical alterations of hippocampal pyramidal neurons: Implications for learning and memory. Ageing Res Rev, 2002, 1: 181－207
32 Zhang C F, Du H Z, Yang P. Ion channel hypothesis for molecular mechanism of Alzheimer's disease. Prog Chem, 2006, 18 (9): 1194－1199
33 Cuajungco M P, Faget K Y, Huang X, Tanzi R E, Bush A I. Metal chelation as a potential therapy for Alzheimer's disease. Ann NY Acad Sci, 2000, 920: 292－304